THE ASTROPHYSICAL JOURNAL, 556:L47–L50, 2001 July 20

MID-INFRARED OBSERVATIONS OF THE MIRA CIRCUMSTELLAR ENVIRONMENT

MASSIMO MARENGO, MARGARITA KAROVSKA, GIOVANNI G. FAZIO, AND JOSEPH L. HORA
Harvard-Smithsonian Center for Astrophysics, 60 Garden Street, Cambridge, MA 02138; mmarengo@cfa.harvard.edu
WILLIAM F. HOFFMANN
Steward Observatory, University of Arizona, 933 North Cherry Avenue, Tucson, AZ 85721-0065
ADITYA DAYAL
KLA-Tencor Corporation, 160 Rio Nobles, San Jose, CA 94134
AND
LYNNE K. DEUTSCH
Department of Astronomy, CAS 519, Boston University, 725 Commonwealth Avenue, Boston, MA 02215
Received 2001 June 18; accepted 2001 June 19; published 2001 July 13

ABSTRACT

This Letter presents results from high angular resolution mid-IR imaging of the Mira AB circumbinary environment using the Mid-InfraRed Array Camera MIRAC3 at the NASA Infrared Telescope Facility. We resolved the dusty circumstellar envelope at 9.8, 11.7, and 18 μm around Mira A (o Ceti) and measured the size of the extended emission. Strong deviations from spherical symmetry are detected in the images of the Mira AB system, including possible dust clumps in the direction of the companion (Mira B). These observations suggest that Mira B plays an active role in shaping the morphology of the circumstellar environment of Mira A as it evolves toward the planetary nebula phase.

Subject headings: binaries: close — circumstellar matter — infrared: stars — stars: individual (o Ceti)

1. INTRODUCTION

Mira A (o Ceti, Mira) is a cool pulsating giant of M2-7 III spectral type, with a mass comparable to our Sun and a diameter of several hundred solar radii. A prototype of the Mira-type class of long-period variables, it has a period of 332 days during which its brightness changes by several magnitudes in the optical. Mira has a hot companion (Mira B) at an angular distance of ~0.″6. The companion is probably a white dwarf accreting from Mira's wind (Reimers & Cassatella 1985; Karovska et al. 1997a).

Recent *Hubble Space Telescope* (*HST*) observations detected significant asymmetries in the giant's atmosphere and found evidence for possible interaction with its companion. The *HST* Faint Object Camera optical images showed that the Mira A atmosphere is elongated in the direction of 175° with an apparent size of 56 mas. *HST* UV images showed a "hooklike" structure extending eastward from the Mira A photosphere toward Mira B (Karovska et al. 1997a, 1997b). These results suggest that the companion may have an important role in shaping the circumstellar environment of the system.

Mira A is losing mass via a strong dust-driven wind, at the rate of $\sim 5 \times 10^{-7}\ M_{\odot}\ \mathrm{yr}^{-1}$ (see Loup et al. 1993 and references therein). As a consequence, the star is surrounded by an extended circumstellar envelope of gas and dust. Observations of the Mira A molecular envelope at radio wavelengths show deviations from spherical symmetry (see, e.g., Planesas, Kenney, & Bachiller 1990; Josselin at al. 2000). The dust is revealed via its strong infrared excess (Joint *IRAS* Science Working Group 1986; Gezari et al. 1993), dominated by an emission feature at 10 μm, which identifies an O-rich composition (Monnier, Geballe, & Danchi 1998). Evidence for spatially extended emission from Mira circumstellar dust was first obtained by Bauer & Stencel (1994) while analyzing the *IRAS* satellite data at 60 μm. More recently, mid-IR observations have been performed at 11 μm with the Infrared Spatial Interferometer (ISI), probing the dust distribution at a smaller spatial scale. By fitting the observed visibilities with models, Lopez et al. (1997) inferred the presence of asymmetries and inhomogeneities in Mira's dust envelope.

Mira-type stars are in the asymptotic giant branch (AGB) phase and are among the precursors of planetary nebulae (PNs; see Habing 1990 for a review). The dynamical evolution of AGB circumstellar envelopes is largely controlled by the dust component, which mediates the momentum transfer from the radiation field to the molecular gas. Mapping the spatial distribution of the dust grains in the Mira AB circumbinary environment is thus necessary to understand the future evolution of the system toward the PN phase and the dynamics of the interaction between its two stellar components.

We present here the first subarcsecond mid-IR images of the Mira A circumstellar environment that map the two-dimensional distribution of the dust emission. The observations and the techniques for data acquisition and reduction are presented in § 2. The results are shown in § 3 and discussed in relation to other available observations and models.

2. OBSERVATIONS AND DATA REDUCTIONS

The observations were performed on 1999 September 22 (JD 2,451,444) when the source was at light-curve phase 0.7, close to minimum luminosity, according to the American Association of Variable Stars Observers (AAVSO). We used the Mid-InfraRed Array Camera MIRAC3 (Hoffmann et al. 1998), mounted at the 3.0 m telescope at the NASA Infrared Telescope Facility (IRTF). MIRAC3 uses a Boeing HF16 128 × 128 Si:As blocked impurity band detector. The IRTF MIRAC3 has a plate scale of 0.″34 pixel^{-1}, providing a total field of view of 42″ × 42″. This pixel scale ensures Nyquist sampling of the diffraction-limited point-spread function (PSF).

We obtained images of Mira AB in MIRAC3 9.8, 11.7, and 18.0 μm 10% passband filters, with a total on-source integration time of 1600 s at each wavelength. The reference star α Tau was observed when transiting at a similar air mass of the source, to provide flux and PSF calibration.

We used a standard nodding and chopping technique to re-

TABLE 1
MID-IR PHOTOMETRY AND ANGULAR SIZE

WAVELENGTH (μm)	PHOTOMETRY (Jy)	FWHM RADIAL AVERAGE PROFILE	
		Source (arcsec)	Reference (arcsec)
9.8	2710 ($\pm$135)	1.05	0.97
11.7	2170 ($\pm$110)	1.08	1.01
18.0	2020 ($\pm$270)	1.56	1.32

move the background signal, dithering the source on the array to obtain subsampling of the PSF. The chop frequency was set to 2 Hz, with a throw of 20″ in the north-south direction. The nod throw was also set to 20″, but in the east-west direction, in order to have all four chop-nod beams inside the field of view of the array. Each individual nod cycle required 10 s on-source integration, and the procedure was repeated for as many cycles as needed to obtain the requested total integration time.

The data were analyzed by first subtracting the chop-on from the chop-off frames for both nodding beams. The two images thus obtained were then subtracted one from the other, in order to get a single frame in which the source appears in all four beams (two negative and two positive). We then applied a gain matrix, derived from images of the dome (high-intensity uniform background) and the sky (low-intensity uniform background), to flat-field the chop-nodded image.

This procedure was repeated for each of the nodding cycles for which the source was observed. A final high signal-to-noise ratio (S/N) cumulative image was then obtained by co-adding together all the beams, each recentered and shifted on the source centroid. The last bit of co-adding was performed on a subpixel grid having the size of one-fifth (9.8 and 11.7 μm images) or one-third (18.0 μm image) of the original MIRAC3 pixels, thus providing a final pixel scale of 0.″068 and 0.″114 pixel^{-1}, respectively. A mask file to block out the effects of bad pixels and field vignetting was also created and applied at this stage, preventing individual rejected pixels from contributing to the final image. The same observing and reduction procedure was also used for the reference star, to ensure a uniform treatment of the source and the standard.

3. RESULTS AND DISCUSSION

3.1. *Source Photometry*

We first estimated the brightness of Mira AB using the multiwavelength co-added images. The aperture photometry at the three observed wavelengths yields ~2710 Jy at 9.8 μm, ~2170 Jy at 11.7 μm, and ~2020 Jy at 18.0 μm (see Table 1). Photometric errors are on the order of 5% at 9.8 and 11.7 μm and 8% at 18.0 μm.

Our measurements are consistent with the published mid-IR fluxes of the source (Gezari et al. 1993), which are in the range 1300–5400 Jy at ~10 μm, 1500–5500 Jy at 11–12 μm, and 1100–2800 Jy around 18 μm. This wide spread, in part due to the large uncertainties of the published data, is a consequence of the source long-period variability, which is still present at infrared wavelengths. Note that, in the mid-IR, only a small fraction of the overall luminosity is contributed by Mira A stellar flux, due to the greater brightness of the dust envelope. The observed infrared variability is thus affected by the changes in the physical and thermodynamical status of the circumstellar dust.

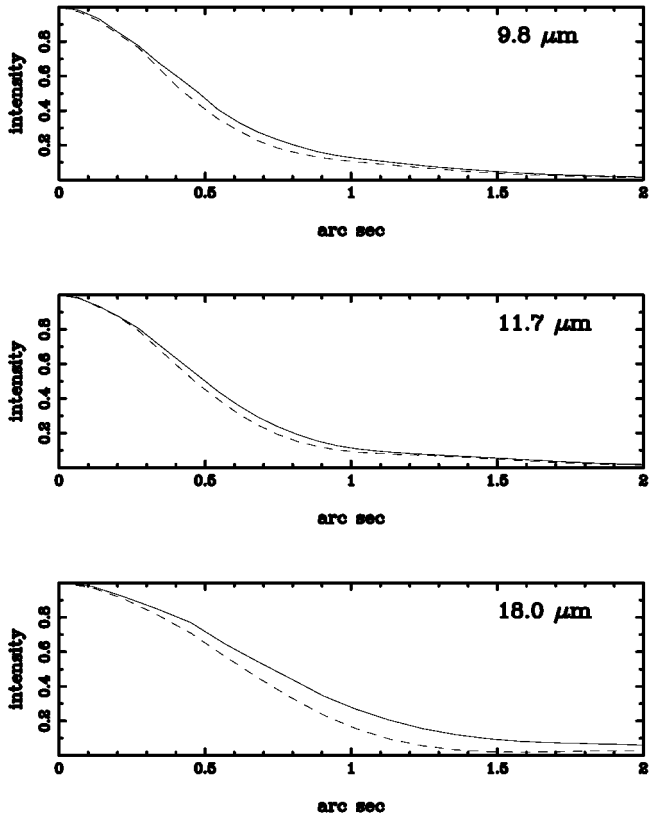

FIG. 1.—Radial profiles of the Mira AB image (*solid line*) and of the reference image (*dashed line*) at 9.8, 11.7, and 18.0 μm.

3.2. *Size of Mira's Dust Envelope*

Our images of Mira AB at 9.8, 11.7, and 18.0 μm indicate that the dusty envelope is spatially resolved at all observed wavelengths. This is shown in Figure 1, which plots the azimuthal averages of the source and reference (radial profiles), normalized at the same peak value. In all panels the source profile has a larger FWHM than the reference star (assumed to be a point source), which is a clear indication of spatial extension. The measured FWHMs are listed in Table 1.

We estimated the apparent size of the Mira AB envelope as a function of wavelength by convolving the reference star profile with a Gaussian model of the Mira A envelope and then fitting to the source radial profile. We obtained an FWHM of 0.″34, 0.″35, and 0.″86 for the best-fit Gaussian model at 9.8, 11.7, and 18.0 μm, respectively. As expected, the apparent sizes of Mira are almost the same at 9.8 and 11.7 μm. The Mira A envelope is significantly larger at 18 μm. We obtained very similar results using deconvolved images described in § 3.3. Using a *Hipparcos* measured distance of 128 pc (Perryman et al. 1997), we estimate the apparent spatial scale of the Mira A dust envelope from 50 AU (at 10 μm) to 100 AU at 18 μm.

The measured apparent sizes of the dust envelope are 10–20 times larger then the apparent size of the Mira A photosphere. For example, the mid-infrared observations using the ISI resolved the Mira A stellar photosphere, measuring a uniform disk diameter of 47.8 mas (Weiner et al. 2000).

The larger size of the 18 μm envelope can be explained on the basis of the radiative transfer properties of AGB envelopes, which in general have a radial thermal structure that can be approximated with a power law $T \propto r^{-0.4}$ (Ivezić & Elitzur

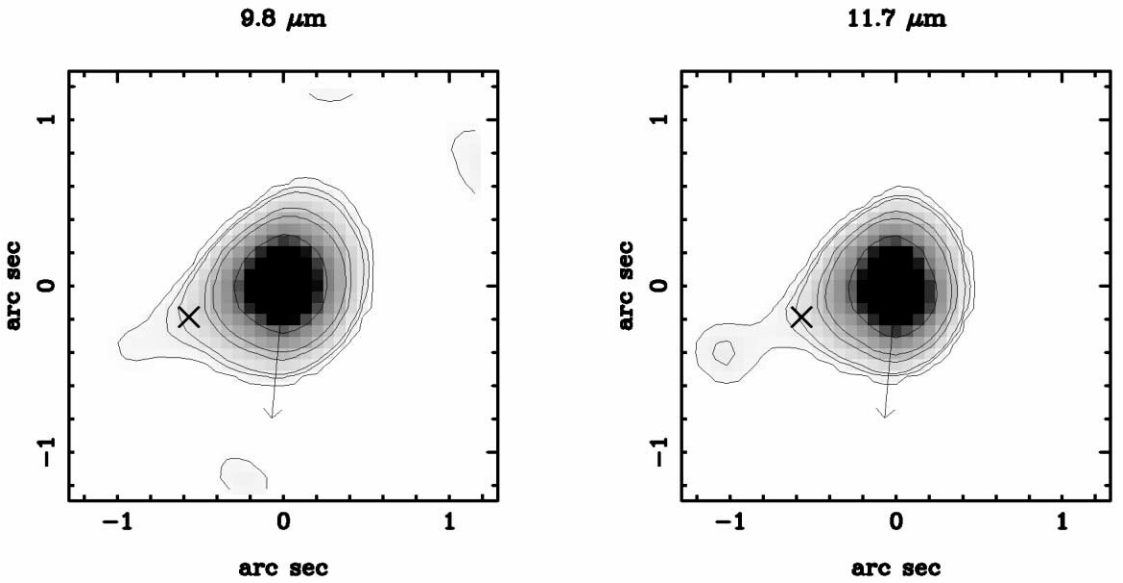

FIG. 2.—Deconvolved images of Mira AB at 9.8 and 11.7 μm. North is up, and west is to the right. The location of Mira B, as observed by *HST* in 1995, is marked by a cross; the arrow indicates the orientation of the dominant asymmetry in the 1995 *HST* image of Mira A (Karovska et al. 1997a). The contours are plotted for 0.001, 0.005, 0.01, 0.05, 0.1, and 0.5 of the maximum flux density level.

1997). Since the peak of emission for the dust radiation at a certain wavelength is inversely proportional to the grain temperature (Wien's law), one should expect $T_{18\,\mu\mathrm{m}}/T_{11.7\,\mu\mathrm{m}} \simeq 0.65$. This means that the size of the region where most of the 18 μm flux is produced should be $r_{18\,\mu\mathrm{m}} \simeq 2.9 r_{10\,\mu\mathrm{m}}$. This factor is similar to the measured ratio between the FWHM of the 18.0 and 11.7 μm deconvolved images (~2.5) and much larger than the PSF spread due to the telescope resolving power (proportional to λ, e.g., ~1.5). Note that this calculation is only a rough estimate for the real size of the envelope. Better estimates can be obtained using models including physical parameters such as the dust condensation radius. This requires a simultaneous fitting of the radial intensity profile and the source spectral energy distribution, which allows derivation of the envelope optical depth τ_V and the inner shell temperature T_1 (Marengo, Ivezić, & Knapp 2001). Results using these models will be presented in a separate paper.

3.3. *Envelope Asymmetries*

Our multiwavelength direct mid-IR images show asymmetries that are not seen in the images of the reference star taken with the same filters. We confirmed the presence of significant departures from spherical symmetry in Mira's dust envelope by performing deconvolution using the Richardson-Lucy method (Richardson 1972; Lucy 1974). The images at 9.8 and 11.7 μm were deconvolved with the corresponding reference star images used as PSFs. This technique was not applied to the 18.0 μm image due to the lower S/N of the source/reference pair.

The deconvolved images are similar at 9.8 and 11.7 μm, as shown in Figure 2. They show that the spatial distribution of the dust in the Mira A circumstellar environment is clearly not spherical. Two dominant asymmetries are detected in the images: one with a major-axis position angle of 175° and another at a position angle of approximately 110°.

The first asymmetry is in the same direction as the asymmetry in the Mira A TiO envelope observed with *HST* in 1995 (Karovska et al. 1997a), but its apparent size is roughly 10 times larger then the one measured in the *HST* images. Near-IR images obtained in the *JHK* bands by Cruzalèbes et al. (1998) also show a north-south elongated shape, which has been interpreted as scattered light from dust. The observed asymmetries could be due to an asymmetric outflow, as suggested by Planesas et al. (1990) and Josselin at al. (2000).

The second dominant asymmetry in Mira AB mid-IR images is in the direction of the companion. This is in agreement with earlier mid-IR observations suggesting the presence of an eastward asymmetry (Lopez et al. 1997; M. Meixner 2000, private communication). Figure 2 shows the location of the companion as observed by *HST* in late 1995 (Karovska et al. 1997a). We do not expect that the position angle and the separation of the companion have changed substantially since 1995, because of its long orbital period of several hundred years (Baize 1980). Our images indicate that the companion is embedded in the elongated dust envelope of Mira A. Because of the limited angular resolution in these observations, we cannot determine if the asymmetry is due to a second unresolved clump located in the vicinity of the companion or is a continuous extension of the Mira A dust envelope toward the companion.

Furthermore, a fainter clump slightly above the noise level is resolved at a distance of 1.″1 from the main source, with a position angle of 115°. Its brightness is ~14.0 ± 1.5 Jy at 9.8 μm and ~11.0 ± 1.0 Jy at 11.7 μm, which is a factor of ~200 fainter than the main source. We estimate a color temperature of 390 ± 100 K, obtained by blackbody fitting of the clump brightness at the two observed wavelengths. The presence of dust clumps has been suggested by interferometric observations using the ISI 11 μm visibilities by Lopez et al. (1997). Their "Clump 3" model, in particular, invokes the presence of dust clumps with a position angle of 120°, which may thus be associated with our observed structures.

The mid-IR observations of Mira AB system indicate that the shape of the Mira A circumstellar envelope may be directly influenced by the presence of the companion orbiting the main AGB mass-losing star. Hydrodynamic models in dusty winds of close binary systems (Mastrodemos & Morris 1999) predict the formation of spiral shocks in the orbital plane, which trail

and follow the secondary star. The structures observed in the mid-IR may be related to this kind of phenomenon. However, the interpretation of the observed geometry is still open, given that the dynamics of the interactions between the two components of close binary systems is not well understood.

4. CONCLUSIONS

Our mid-IR images of the Mira AB dust envelope show significant departures from spherical symmetry. They also indicate that the overall distribution of the circumstellar dust is affected by the presence of a companion. Given the role of dust in shaping the future dynamical evolution of the system, these observations not only give a better characterization of the geometry of the Mira AB binary system but may also contribute to a better understanding of the formation of asymmetric PNs.

Many details of the transition from the AGB to PN cannot be explained on the basis of the spherically symmetric "interacting stellar winds" theory (Kwok, Purton, & Fitzgerald 1978), which defines the general framework of PN formation. High-resolution *HST* images of PNs reveal a general absence of spherical symmetry, in favor of bipolar structures enriched by a multitude of microstructures (jets, clumps, "fliers," etc.). Optical and mid-IR post-AGB and pre-PN images (Sahai et al. 1998; Meixner et al. 1999; Ueta, Meixner, & Bobrowsky 2000) show envelope asymmetries already present before the onset of the PN phase. How these structures evolve is unknown. The results of our IR observations show that Mira AB offers the possibility of observing the beginning of this process.

We thank the IRTF staff for their outstanding support. M. K. is a member of the *Chandra* Science Center, which is operated under contract NAS8-39073 and is partially supported by NASA. We also thank the referee for his/her useful comments.

REFERENCES

Baize, P. 1980, A&AS, 39, 83
Bauer, W. H., & Stencel, R. E. 1994, AJ, 107, 2233
Cruzalèbes, P., Lopez, B., Bester, M., Gendron, E., & Sams, B. 1998, A&A, 338, 132
Gezari, D. Y., Schmitz, M., Pitts, P. S., & Mead, J. M. 1993, Catalog of Infrared Observations (3d ed., NASA RP-1294; Washington, DC: NASA)
Habing, H. J. 1990, in From Miras to Planetary Nebulae: Which Path for Stellar Evolution?, ed. M. O. Mennessier & A. Omont (Gif-sur-Yvette: Editions Frontières), 16
Hoffmann, W. F., Hora, J. L., Fazio, G. G., Deutsch, L. K., & Dayal, A. 1998, Proc. SPIE, 3354, 647
Ivezić, Ž., & Elitzur, M. 1997, MNRAS, 287, 799
Joint *IRAS* Science Working Group. 1986, *IRAS* Catalogs and Atlases (Washington, DC: NASA)
Josselin, E., Mauron, N., Planesas, P., & Bachiller, R. 2000, A&A, 362, 255
Karovska, M., Hack, W., Raymond, J., & Guinan, E. 1997a, ApJ, 482, L175
Karovska, M., et al. 1997b, NASA and STScI press release, STScI-PRC97-26
Kwok, S., Purton, C. R., & Fitzgerald, P. M. 1978, ApJ, 219, L125
Lopez, B., et al. 1997, ApJ, 488, 807
Loup, C., Forveille, T., Omont, A., & Paul, J. F. 1993, A&AS, 99, 291
Lucy, L. B. 1974, AJ, 79, 745
Marengo, M., Ivezić, Ž., & Knapp, G. R. 2001, MNRAS, 324, 1117
Mastrodemos, N., & Morris, M. 1999, ApJ, 523, 357
Meixner, M., et al. 1999, ApJS, 122, 221
Monnier, J. D., Geballe, T. R., & Danchi, W. C. 1998, ApJ, 502, 833
Perryman, M. A. C., et al. 1997, A&A, 323, L49
Planesas, P., Kenney, J. D. P., & Bachiller, R. 1990, ApJ, 364, L9
Reimers, D., & Cassatella, A. 1985, ApJ, 297, 275
Richardson, W. H. 1972, J. Opt. Soc. Am., 62, 55
Sahai, R., et al. 1998, ApJ, 493, 301
Ueta, T., Meixner, M., & Bobrowsky, M. 2000, ApJ, 528, 861
Weiner, J., Danchi, W. C., Hale, D. D. S., McMahon, J., Townes, C. H., Monnier, J. D., & Tuthill, P. G. 2000, ApJ, 544, 1097